Maslakov, K. I., Teterin, Y. A., Popel, A. J., Teterin, A. Y., Ivanov, K. E., Kalmykov, S. N., ... Farnan, I. (2018). XPS study of the surface chemistry of UO_2 (111) single crystal film. *Applied Surface Science*, *433*, 582-588. https://doi.org/10.1016/j.apsusc.2017.10.019

Applied Surface Science 433 (2018) 582–588

Contents lists available at ScienceDirect

Applied Surface Science

journal homepage: www.elsevier.com/locate/apsusc

Full Length Article

XPS study of the surface chemistry of UO_2 (111) single crystal film

Konstantin I. Maslakov[a], Yury A. Teterin[a,b], Aleksej J. Popel[c,d,*], Anton Yu. Teterin[b], Kirill E. Ivanov[b], Stepan N. Kalmykov[a,b], Vladimir G. Petrov[a], Ross Springell[e], Thomas B. Scott[e], Ian Farnan[c]

[a] Chemistry Department, Lomonosov Moscow State University, Moscow, 119991, Russia
[b] NRC "Kurchatov Institute", Moscow, 123182, Russia
[c] Department of Earth Sciences, University of Cambridge, Downing Street, Cambridge, CB2 3EQ, UK
[d] Department of Materials, Imperial College London, London, SW7 2AZ, UK
[e] Interface Analysis Centre, School of Physics, University of Bristol, Bristol, BS8 1TL, UK

ARTICLE INFO

Article history:
Received 11 May 2017
Received in revised form
15 September 2017
Accepted 4 October 2017
Available online 8 October 2017

Keywords:
XPS
Ar sputtering
UO_2
Thin film
Surface chemistry
Ionic composition

ABSTRACT

A (111) air-exposed surface of UO_2 thin film (150 nm) on (111) YSZ (yttria-stabilized zirconia) before and after the Ar^+ etching and subsequent in situ annealing in the spectrometer analytic chamber was studied by XPS technique. The U 5f, U 4f and O 1s electron peak intensities were employed for determining the oxygen coefficient $k_O = 2 + x$ of a UO_{2+x} oxide on the surface. It was found that initial surface (several nm) had $k_O = 2.20$. A 20 s Ar^+ etching led to formation of oxide $UO_{2.12}$, whose composition does not depend significantly on the etching time (up to 180 s). Ar^+ etching and subsequent annealing at temperatures 100–380 °C in vacuum was established to result in formation of stable well-organized structure $UO_{2.12}$ reflected in the U 4f XPS spectra as high intensity (~28% of the basic peak) shake-up satellites 6.9 eV away from the basic peaks, and virtually did not change the oxygen coefficient of the sample surface. This agrees with the suggestion that a stable (self-assembling) phase with the oxygen coefficient $k_O \approx 2.12$ forms on the UO_2 surface.

1. Introduction

The data on UO_2 stability, stoichiometric and ionic composition are important for uranium ore extraction [1], spent fuel storage and disposal, as well as for remediation of uranium contaminated environments [2–4]. Uranium oxide solubility depends strongly on uranium oxidation state. U^{6+} compounds are much more soluble than U^{4+} ones [5]. Therefore, oxidation state of uranium ions in spent nuclear fuel correlates with solubility and corrosion rate [6], which determines the release rate of the majority of radionuclides [7].

Polycrystalline uranium dioxide is known almost always to contain excessive oxygen. Its general formula is UO_{2+x} ($x > 0.01$). As oxygen excess grows, UO_2 cell shrinks to $a_x = 5.4690 - 0.12x$ [8]. For example, $UO_{2.12}$ phase is suggested to correspond to stoichiometric composition of oxide U_8O_{17} with $a_0 = 5.456$ Å. UO_2 oxidation in the air starts with oxygen absorption on the grain surface. Oxygen included in UO_2 lattice after diffusion can take intermediate positions like (½00) in the edges and (½½½) in the center of the unit cell. Getting these vacancies filled, the unit cell can reach the composition of UO_3, but at relatively low temperatures the actual saturation limit does not exceed $UO_{2.30}$ [8]. On the further filling, the tetragonal phase forms. Intrusion of oxygen ions in UO_2 lattice accompanied by the UO_2 lattice contraction is only possible if uranium ions oxidize from U^{4+} to U^{5+} and U^{6+}, i.e. uranium ionic radii decrease as UO_2^+ and UO_2^{2+} ions form [8]. Therefore, a complex oxide UO_{2+x} was suggested to form on the surface of single crystal UO_2 film in an atmospheric air [9]. Stability of a cubic-octahedral cluster U_6O_{12} was theoretically studied [10]. This cluster can form in non-stoichiometric oxides UO_{2+x}. Such a structural stability is inherited from the molecular cluster U_6O_{12}.

X-ray and other spectra determination of stoichiometric composition of standard complex oxides UO_{2+x} require single crystal uranium oxide films. This provides correct high-resolution spectra and reliable results [9,11–13]. Therefore, the technique of film preparation and study is a question of a special attention [9,12,14–16].

Photoemission spectroscopy (PES) [11,17–19] and X-ray photoelectron spectroscopy (XPS) [4,11,20,21] are widely used for ionic

* Corresponding author. Present address: Department of Earth Sciences, University of Cambridge, Downing Street, Cambridge, CB2 3EQ, UK.
E-mail address: apopel@cantab.net (A.J. Popel).

https://doi.org/10.1016/j.apsusc.2017.10.019

characterization of uranium oxides UO_{2+x}. These methods are also used for uranium oxide surface characterization on various substrates [11–13,22,23]. The work in Ref. [11] considers the U 4f and O 1s XPS spectra structure of oxide row UO_{2+x} under different etching and annealing conditions.

The determination of the uranium oxidation state employs the spectrum of the U 4f-electrons [20,24]. The binding energy (BE) of the U $4f_{7/2}$ electrons grows with an increase of the uranium oxidation state in oxides [12,20,24–26]. A special attention was paid to the study of the mechanisms of structure formation, which leads to widening of the main peaks and appearance of additional structure in the spectra [20,27–31]. The XPS spectra of the U 4f-electrons of some oxides exhibit typical shake-up satellites [18,20,23]. Relative satellite intensity I_{sat} (%) is calculated as a ratio of satellite intensity (I_s) to the basic peak intensity (I_o) [11,23]. The mechanisms of the shake-up satellite appearance are considered in Refs. [20,30]. The U 4f XPS structure is best resolved for single crystal oxide films. The U 4f spectrum from complex amorphous oxides UO_{2+x} is often hard to separate unambiguously into components. This does not allow reliable quantitative information on uranium oxidation state and ionic composition.

The earlier paper (Ref. [32]) noted that Ar^+ etching of the (111) surface of the studied single crystal film caused a formation of an n-type semiconductive UO_{2-x} phase. Upon a 527 °C annealing at 5×10^{-6} mbar of O_2 a p-type semiconductive UO_{2+x} phase forms. The UO_2 phase is a Mott-Hubbard insulator [2].

A short-time etching causes an increase in the satellite intensity at 6.9 eV in the U 4f XPS spectrum and appearance of the peaks attributed to metallic uranium form at the lower BE side from the basic oxide peak. The O 1s, 2s intensity drops, and the U 5f intensity grows during the etching [32–34].

The goal of this work was to study uranium dioxide surface after etching and annealing. Therefore, the main attention was focused on the main XPS parameters of both core and valence electrons such as: binding energy; structure of the inner and outer valence molecular orbitals; intensities and position of shake-up satellites; intensities and widths of the U 4f, U 5f and O 1s peaks.

As a result, the structure of the XPS spectra of the valent and inner electrons on the surface of uranium dioxide film was studied in this work. For this purpose a thin (150 nm) UO_2 film on the YSZ (yttria-stabilized zirconia) substrate was prepared and the XPS study of the (111) surface of the film was done, the influence of Ar^+ etching and annealing was studied. The film was studied before and after the Ar^+ etching and annealing (in situ) at various times of etching and annealing.

2. Experimental section

2.1. Thin film production

Epitaxial thin film (150 nm) of UO_2 with (111) surface orientation (Fig. 1) was produced by reactive sputtering onto YSZ (111) substrate at the University of Bristol and thoroughly characterized in Refs. [9,15]. A dedicated DC magnetron sputtering facility with UHV base pressure (10^{-9} mbar) was employed to grow the film. The YSZ substrate was kept at the temperature close to 600 °C.

2.2. X-ray photoelectron measurements

After contact with atmosphere UO_2 thin film, denoted UO_{2+x}, have been analyzed by XPS using a Kratos Axis Ultra DLD spectrometer. The quantitative elemental analysis was performed for the surface of the studied sample as it was described in [9]. The error in the determination of the BE and the peak width did not exceed ±0.05 eV, and the error of the relative peak intensity was

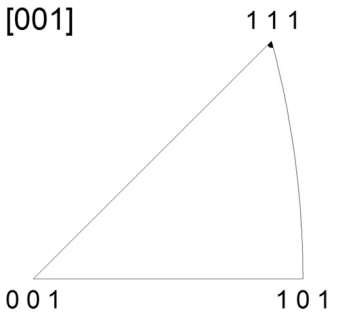

Fig. 1. A triangular inverse pole figure diagram for sample AP7(0) obtained from the EBSD study (Ref. [15]).

±5% [9]. The inelastically scattered electrons-related background was subtracted by the Shirley method [35].

$^{40}Ar^+$ etching of 2×2 mm^2 sample area was conducted at the accelerating voltage of 2 kV and current density of 25 μA/cm^2 at 2×10^{-9} mbar and room temperature for 20, 60, 120 and 180 s. The sputtering took place in the same place consequently after acquiring sequential group of spectra according to the scheme: 20 + 40 + 60 + 60 s (180 s in total). The etching rate under these conditions for SiO_2 was 7.1 nm/min. The ion flux was kept at $\sim 1.5 \times 10^{14}$ ions/(cm^2 s).

To study the surface (the first ~5 nm [36]) of the film, etching and annealing of the sample were performed. Sample AP7(0) was annealed in the spectrometer preparation chamber at 600 °C for 1 h in order to outgas the sample and the sample holder before the experiment. The U 4f spectrum of UO_{2+x} did not change significantly after the annealing. Afterwards the sample was etched with argon ions and annealed in the analytical chamber of the spectrometer. During this process the XPS spectra were collected from the same spot on the sample surface.

2.3. Determination of the oxygen coefficient $k_O = 2 + x$ of oxides UO_{2+x}

There are known two methods for determining the oxygen coefficient $k_O = 2 + x$ and ionic composition in complex UO_{2+x} oxides based on XPS data [20,37]. The first method uses line intensities and binding energies of the inner U 4f- and O 1s-electrons with photoemission cross-sections of these electrons. The magnitudes of the photoemission cross-sections are determined by calculations [38–40]. The second method is based on the relative intensity of the U 5f-electrons line, which is equal to the ratio of U 5f- and U $4f_{7/2}$-electron intensities. This technique is described in detail in Ref. [9]. In the current work we provide only the main Eq. (1) for determination of the k_O. The U 5f intensity I_1 (rel. units) determined as the U 5f/U $4f_{7/2}$ intensity ratio without the shake-up satellites can be presented as:

$$I_1 = 5.366\, k_O^{-7.173}. \quad (1)$$

3. Results and discussion

As mentioned before, determination of uranium oxidation state and UO_{2+x} ionic composition employs both the traditional XPS parameters (BEs and peak intensities) and the structure parameters of the core- and valence spectra. These XPS parameters allow getting information on uranium physical and chemical properties in the studied sample. The XPS survey-scan of a (111) surface of UO_{2+x} single crystal thin film (150 nm) on (111) YSZ (yttria-stabilized zirconia) is shown in Fig. 2. It does not differ much from the corresponding spectrum of a (001) surface of UO_{2+x} single crystal thin film (120 nm) on (001) LSAT (lanthanum strontium aluminum tan-

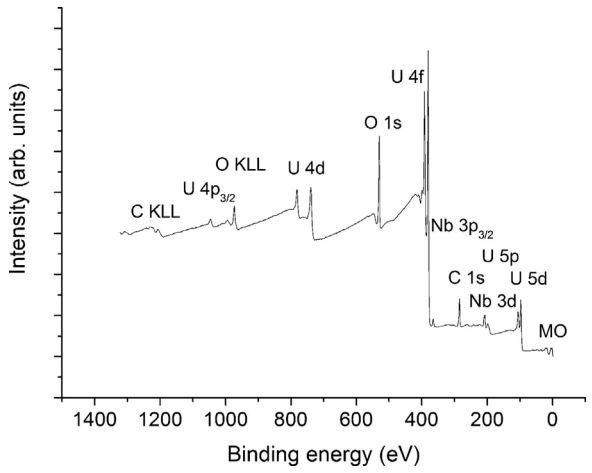

Fig. 2. Survey XPS scan of UO_{2+x} sample AP7(0).

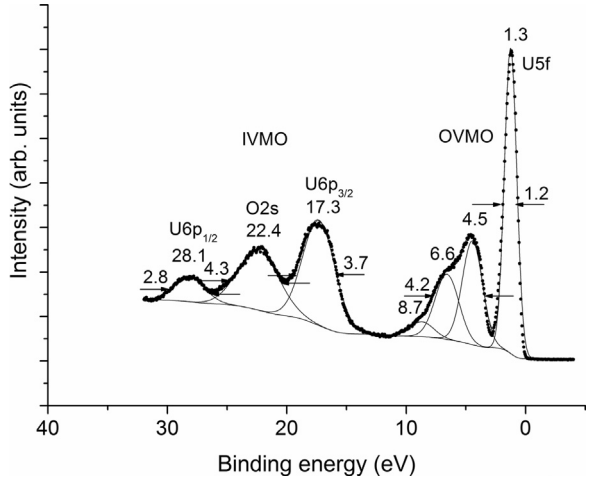

Fig. 3. XPS scans of valence electrons of the UO_{2+x} film after Ar^+ etching and 1 h annealing at 380 °C AP7(60).

talum oxide) in Ref. [9] despite the difference in the crystallographic orientation of the surface and different substrate.

3.1. Valence electron spectra range

Fig. 3 shows the spectrum of valence electrons of the AP7b(60) film after the subsequent 1 h annealing at 380 °C. The observed structure agrees satisfactorily with the calculation results for UO_2 [39]. The region of the valent electrons spectrum consists of two parts.

The first part from 0 to ~15 eV represents the structure related to the electrons of the outer valence molecular orbitals (OVMO). The second part from ~15 to ~35 eV comprised by the structure of the inner valence molecular orbitals (IVMO). The line at 1.3 eV is related to quasi-atomic U 5f-electrons and its intensity proportional to the number of these weakly bound electrons (Fig. 3). It has a maximum intensity in the $U^{4+}(5f^2)O_2$ spectrum and this line is absent in the spectrum of $U^{6+}(5f^0)O_3$ [20]. Usually, the intensity of I_1 (rel. units) is expressed as the ratio of the intensities of the I_1 = U 5f/U $4f_{7/2}$ electron lines. In this case, the oxygen coefficient (k_O) on the surface of a complex oxide UO_{2+x} (Table 1) can be determined using Eq. (1) and other equations of the technique described in Ref. [9]. For example, for sample AP7(0): I_1 = 0.019; k_O = 2.20 and k(%) equals to 18% (U^{4+}), 61% (U^{5+}) and 21% (U^{6+}) [9].

Table 1
Summary of the elemental (U, O) composition of the UO_{2+x}[b] film surface, intensity line I_1 of U 5f-electrons[c], oxygen coefficient k_O[c] in UO_{2+x} oxide in uranium oxide sample AP7.

Sample (t, s)[a]	Composition UO_{2+x}[b]	I_1[c] (±0.001)	k_O[d] in UO_{2+x} (±0.01)
AP7(0)	$UO_{3.62}$	0.019	2.20
AP7(20)	$UO_{2.51}$	0.025	2.11
AP7(60)	$UO_{2.19}$	0.023	2.14
AP7(120)	$UO_{2.06}$	0.024	2.12
AP7(180)	$UO_{1.98}$	0.025	2.11
AP7b (60) 380 °C, 1 h	$UO_{2.53}$	0.023	2.14
AP7c (30) 100 °C, 30 min	$UO_{2.83}$	0.025	2.11
AP7d (30) 250 °C, 30 min	$UO_{3.10}$	0.024	2.12

[a] Ar^+ etching time t (s) of sample AP7(t).
[b] Elemental (U, O) composition based on the intensity of the lines of internal U $4f_{7/2}$- and O 1s-electrons of uranium dioxide and the atomic cross-section photoeffect σ: 2.81(O 1s), 36.0 (U $4f_{7/2}$).
[c] The intensity of the line of U 5f-electrons measured as a ratio: $I_1 = I_{U5f}/I_{U4f7/2}$.
[d] Oxygen coefficient $k_O = 2 + x$ in UO_{2+x} oxide calculated from Eq. (1).

The spectrum structure of the OVMO electrons is observed as a line with a maximum at 4.5 eV and with a width Γ(OVMO) = 4.2 eV (Fig. 3). In the region of binding energies for the electrons of IVMO there are three widened lines with maxima at 17.3 (3.7), 22.4 (4.3) and 28.1 (2.8) eV. In Fig. 3 these lines are formally assigned to U $6p_{3/2}$-, O 2s- and U $6p_{1/2}$-electrons. If these lines were from the electrons of atomic levels, then the ratio of their intensities would have been approximately equal to the ratio of photoionization cross-sections $\sigma(U\,6p_{3/2})/\sigma(U\,6p_{1/2}) = 2.89$ [40]. However, the ratio of the intensities of these lines is equal to 5.67 (Fig. 3). This difference arises from the fact that these lines represent the spectrum of the IVMO electrons.

Ar^+ etching is known to remove the surface atoms and to break the chemical bonds and the crystal structure [38]. In this case the XPS structure of the valence and the core electrons changes significantly. For example, the XPS of the solid VIA elements exhibits a single ns-peak [41] after an Ar^+ treatment instead of two IVMO peaks due to the ns-ns overlapping.

A short-time Ar^+ etching of AP7(0) leads to increase of the U 5f intensity, as well as the U 5f peak widening and shift to the lower BE side (Tables 1 and 2) due to the increase of the U^{4+} concentration and decrease of the U^{5+} and U^{6+} concentration on the surface.

After the 20 and 60 s argon treatment the OVMO XPS of AP7(0) exhibits the structure with three peaks at 4.5, 6.6 and 9.1 eV, and the IVMO bands narrow (Fig. 4). During this treatment the oxygen coefficient k_O decreases, as compared to the initial sample AP7(0) (Table 1). In the beginning of the etching the U 5f intensity I_1 (Fig. 4, Table 1) and FWHM Γ(U 5f) (Table 2) grow and then remain constant within the measurement error. The subsequent annealing at 100 °C to 250 °C leads to narrowing of the U 5f peak (Fig. 4, Table 2) but does not affect significantly its intensity (Table 1). The annealing at 380 °C leads to narrowing of the U 5f peak and widening of the OVMO bands to the values corresponding to the initial sample AP7(0).

On the basis of this, one can suggest that the 180 s Ar^+ treatment of the UO_{2+x} film on the (111) YSZ substrate in the spectrometer chamber leads only to formation of self-organized stable UO_{2+x} phase with the oxygen coefficient $k_O \approx 2.11$. This agrees with the formula U_nO_{2n+1} for stable oxides at $n = 8$ ($k_O = 2.125$) [8]. The annealing of the samples leads to narrowing of the U 5f peak but does not affect significantly its intensity. This suggestion agrees with the XRD data [42]. Formation of a stable self-organized phase containing the An^{4+} ions during the Ar^+ etching was observed for NpO_2 [43] and PuO_2 [44] films. Ar^+ etching of AmO_2 film leads mostly to formation of the Am^{3+} ions on the surface [45].

Table 2
Summary of the Ar^+ etching time t (s), binding energies E_b[a] (eV), FWHMs Γ(eV)[b], relative intensities of the: O 1s-peak of the basic n_{O1s}[c] and impurity n'_{O1s}[d] oxygen; n_{C1s}[e] and Ar^+ etching time t(s).

Sample (etching time, s)	$E_b(\Gamma)$ U 5f	E_b (Γ) U $4f_{7/2}$	Γ U $4f_{7/2}$	E_b (Γ) O 1s	n_{O1s}	n'_{O1s}	n_{C1s}
AP7(0)	1.5 (1.1)	380.0 (1.5)	2.4	530.1 (1.1)	3.62	0.53	3.01
		381.2 (1.5)		531.4 (1.1)			
		382.7 (1.5)		532.2 (1.1)			
AP7(20)	1.1 (1.5)	379.7	1.8	529.9 (1.3)	2.51	0.26	0.18
		6.9 s[g]		531.5 (1.3)			
AP7(60)	1.1 (1.5)	379.8	1.6	529.9 (1.2)	2.19	0.28	0.17
		6.9 s		531.5 (1.2)			
AP7(120)	1.2 (1.6)	379.8	1.5	530.0 (1.2)	2.06	0.32	0.01
		6.9 s		531.4 (1.3)			
AP7(180)	1.2 (1.6)	379.8	1.6	530.0 (1.2)	1.98	0.31	0.01
		6.9 s		531.4 (1.5)			
AP7b(60) (380 °C, 1 h)[f]	1.3 (1.2)	380.0	1.8	530.2 (1.1)	2.53	0.56	0.91
		7.0 s		531.5 (1.5)			
AP7c (30) (100 °C, 30 min)[f]	1.3 (1.5)	380.0	1.7	530.2 (1.3)	2.83	0.43	0.27
		6.9 s		531.5 (1.5)			
AP7d (30) (250 °C, 30 min)[f]	1.3 (1.2)	380.0	1.7	530.1 (1.1)	3.10	0.58	0.57
		7.0 s		531.4 (1.5)			

[a] BEs are given relative to the E_b(C 1s) = 285.0 eV.
[b] FWHMs are given in the parenthesis relative to the Γ(C 1s) = 1.3 eV.
[c] The number of oxygen (n_{O1s} is oxygen at 530.1 eV, n'_{O1s} is impurity oxygen at 531 eV) and carbon atoms per one uranium atom.
[d] The number of oxygen (n_{O1s} is oxygen at 530.1 eV, n'_{O1s} is impurity oxygen at 531 eV) and carbon atoms per one uranium atom.
[e] The number of oxygen (n_{O1s} is oxygen at 530.1 eV, n'_{O1s} is impurity oxygen at 531 eV) and carbon atoms per one uranium atom.
[f] Annealing temperature and time.
[g] Shake-up satellite.

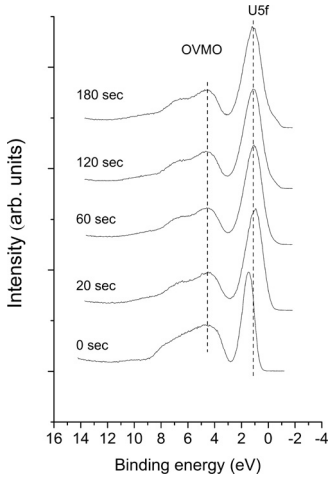

Fig. 4. XPS scans of valence electrons of sample AP7(t) before and after Ar^+ etching at different time.

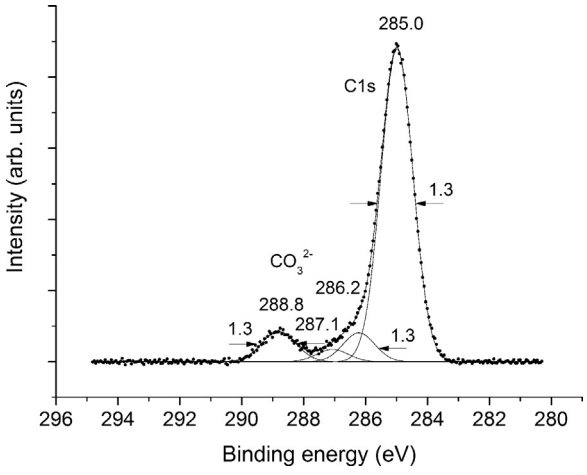

Fig. 5. XPS narrow scan of C 1s on the surface of AP7(0).

3.2. Core electron XPS range

The C 1s XPS spectrum of UO_{2+x} surface consists of the basic peak at E_b = 285.0 eV (saturated hydrocarbons) used for BE calibration [46]. Peaks at 286.2 and 287.1 eV are due to hydrocarbon bound with oxygen, and a peak at 288.8 eV is due to the carbonate group CO_3^{2-} or carboxyl group —COO^- on the surface (Fig. 5). After the 20 s Ar^+ etching the C 1s intensity drops significantly (Table 2).

The O 1s spectrum of the initial sample AP7(0) consists of a relatively sharp basic peak at E_b(O 1s) = 530.1 eV, Γ(O 1s) = 1.1 eV and two low-intensity peaks at 531.4 eV and 532.2 eV with relative intensities of 79%, 15% and 6%, respectively. The peak at 531.4 eV can be attributed to the hydroxyl group, and the second one at 532.2 eV – to the CO_3^{2-} group (Fig. 6a, Table 2). The quantitative analysis based on the core U $4f_{7/2}$ and the basic O 1s (530.1 eV BE) peak intensities yielded the oxygen coefficient of 3.62, which exceeds the expected value of 2 (Tables 1 and 2).

The BE of the O 1s basic peak after the etching did not change significantly (Figs. 6b and c, Table 2). In the beginning of the etching the O 1s FWHM slightly increased and afterward did not change significantly, while the intensity of the basic O 1s peak (n_{O1s}) decreased (Table 2). The hydroxyl-related O 1s peak intensity (n'_{O1s}) at 531.4 eV, in the beginning of the etching dropped noticeably and afterward changed insignificantly (Table 2). The amount of oxygen of the basic peak at ~530.0 eV BE on the surface can exceed significantly the coefficient of 2 as in UO_2 (Table 2). The annealing after the etching leads to the increasing of the hydroxyl-related peak intensity, while the BE of the O 1s-electron does not change (Table 2).

The U 4f spectra are given in Fig. 7. After the 20 s Ar^+ etching of sample AP7(0) the U 4f spectrum changed significantly, and the further etching up to 180 s did not cause any significant changes (Fig. 8, Table 2). Firstly, after the 120 s etching a small shoulder associated with the ions of oxidation state lower than U^{4+} at the lower BE side from the basic U $4f_{7/2}$ peak appeared at 377.0 eV (Fig. 8). It slightly grows after the 180 s etching.

Previously this peak was attributed to metallic uranium [11]. Secondly, the XPS peaks narrowed significantly and simpler structure of the satellites was observed (Figs. 7 and 8). This indicates a

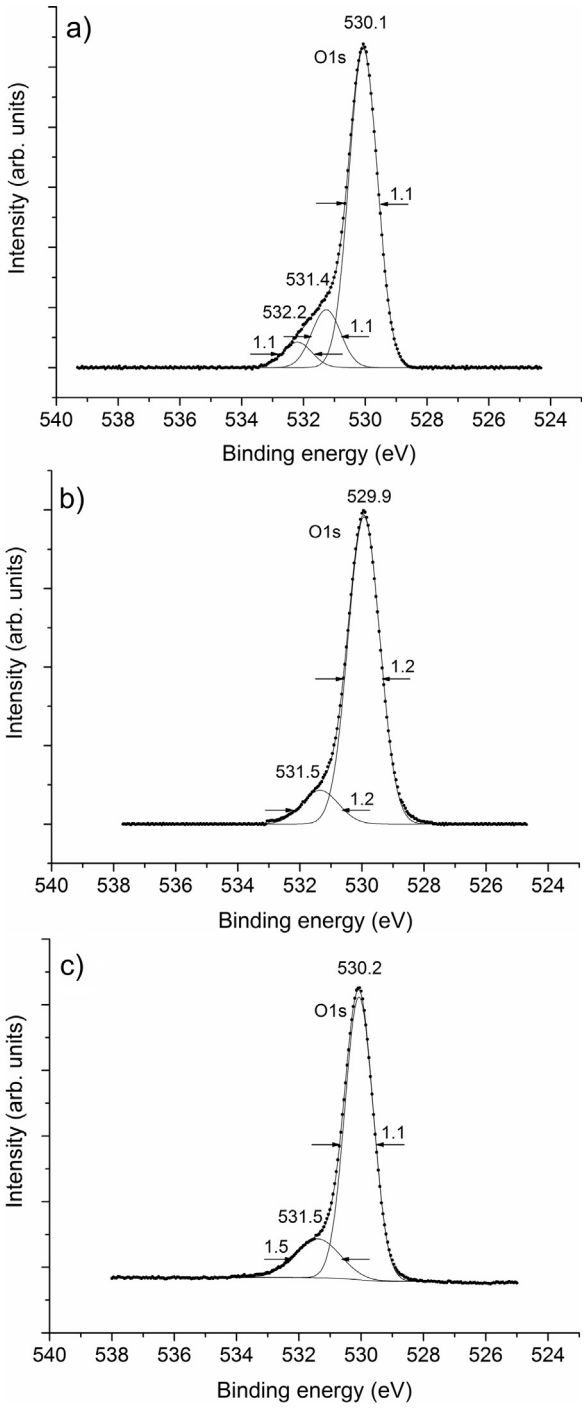

Fig. 6. XPS narrow scans of O 1s: a) initial AP7(0); b) after 60 s Ar^+ etching; c) after Ar^+ etching and 1 h annealing at 380 °C AP7b(60).

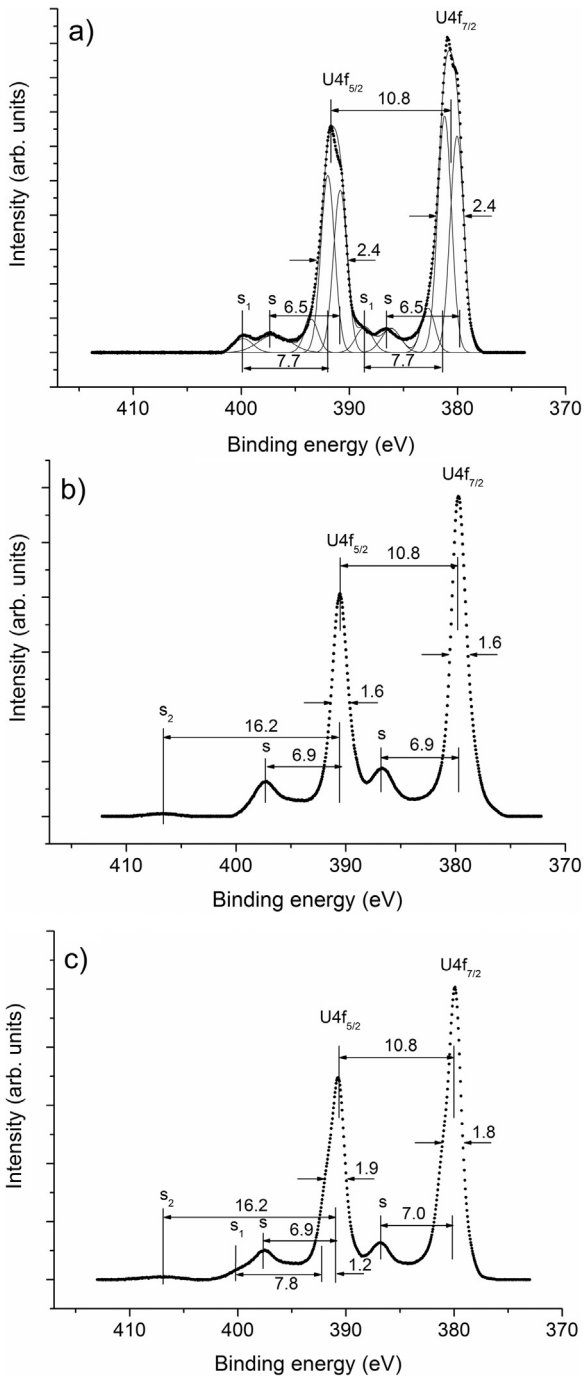

Fig. 7. XPS narrow scans of U 4f: a) initial AP7(0) [9]; b) after 60 s Ar^+ etching; c) after Ar^+ etching for 60 s and 1 h annealing at 380 °C AP7b(60).

chemical bond and a long-range ordering in the lattice that self-organized after the etching in the spectrometer chamber (Fig. 7b). Since the U 4f spectra in this case do not show any explicit peaks attributed to different oxidation states of uranium ions (U^{4+}, U^{5+}, U^{6+}), the decomposition of the spectrum into components is difficult. Therefore, a formal decomposition was done for a qualitative consideration of the ionic composition, and the ionic composition was evaluated only on the basis of the U 5f relative intensity. The technique described in Ref. [9] yields that the considered phase beside the U^{4+} ions, contains U^{5+} and U^{6+} ions.

As it was mentioned above, evaluation of the oxygen coefficient in UO_{2+x} on the basis of the core U $4f_{7/2}$ and O 1s intensities is complicated because of adsorbed oxygen-containing molecules on the surface (Table 1, Figs. 6 and 7). A significant difference in the oxygen coefficient obtained on the basis of the O 1s/U $4f_{7/2}$ intensities and on the basis of the U 5f relative intensity was observed (Table 1).

In order to prepare the sample surface, as it was mentioned, the Ar^+ etching and subsequent annealing of the AP7(0) sample were used. A 1 h annealing of the AP7(0) sample in the spectrometer preparation chamber at 600 °C did not bring any significant changes in the XPS spectra comparing to the initial spectrum (Fig. 7a, Table 2). A 60 s Ar^+ etching lead to formation of oxide $UO_{2.14}$ on the AP7(60) surface, which agrees with the composition $UO_{2.19}$ (Table 1). The further 1 h annealing in the spectrometer analytical chamber at 380 °C leads to formation of oxide $UO_{2.53}$ on the surface

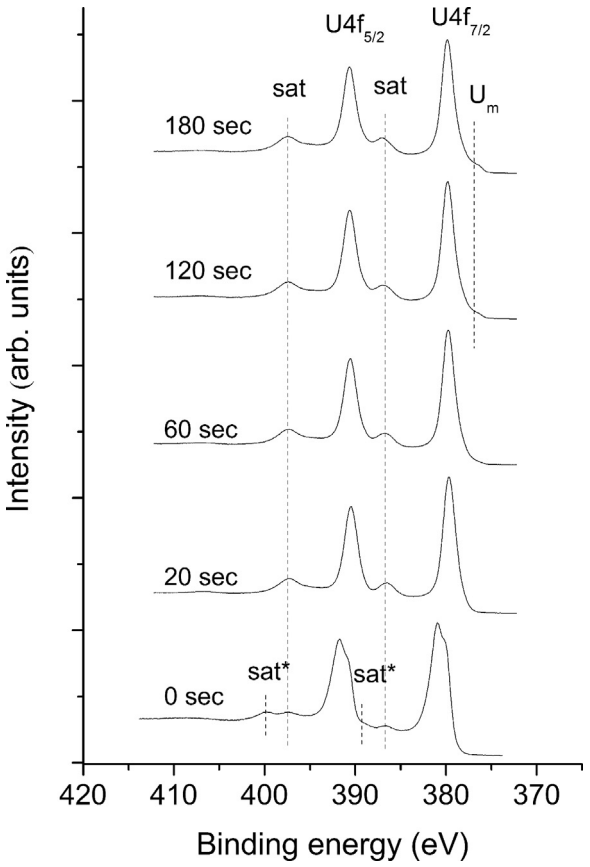

Fig. 8. XPS narrow scans of U 4f of sample AP7(0) after Ar^+ etching t(s).

AP7b(60), which leads to the narrowing of the U 5f peak, widening of the U 4f peak and increasing of oxygen and carbon concentrations on the surface, but does not cause a change in the oxygen coefficient k_O of AP7b(60), as compared to AP7(60) (Tables 1 and 2, Fig. 7c). The U^{5+}-attributed shoulder 1.2 eV away from the basic peak and shake-up satellite appear (Fig. 7c, Table 2). The satellite parameters are sensitive to the ionic composition changes on the surface.

After another 30 s etching oxide $UO_{2.30}$ formed on the AP7(30) surface. The subsequent 30 min annealing at 100 °C, 150 °C, 200 °C and 250 °C under 3.8×10^{-8} mbar in the spectrometer chamber leads to the similar changes in the XPS spectrum of AP7c(30) (Tables 1 and 2). The U 5f intensity I_1 and oxygen coefficient change insignificantly.

An increase of the oxygen content on the surface during the annealing is difficult to explain by oxygen diffusion from the bulk of UO_{2+x}. It is known that oxygen diffusion in UO_2 is low [47]. That is why the oxygen from the 'bulk' would not have time to reach the surface during the annealing [48]. Moreover, the film with a thickness of 150 nm does not contain that much of excessive oxygen. Apparently, during the annealing stage oxygen and oxygen-containing compounds (CO [34], H_2O [49]) desorb from the walls of the spectrometer and adsorb from the surrounding environment on the surface of the sample. Supposedly, this results in formation of complex clusters UO_y^{n-} like $U(CO_3)_2$ and $U(OH)_4$ on the surface, whose O 1s BE is ~531.5 eV (Tables 1 and 2).

During annealing of AP7(60) narrowing of the U 5f peak and widening of the U 4f peak AP7b (Table 2, Fig. 7c) can be explained by an increase in the $U^{5+}(5f^1)$ concentration and a decrease in concentration of the $U^{4+}(5f^2)$ containing two uncoupled U 5f electrons (see AP7(60) and AP7b(60), Table 1). However, from the data for samples AP7(60) and AP7b(60) it follows that the k_O practically does not change on the annealing (Table 2). The U 5f and the U 4f FWHM turn out to be more sensitive to the ionic compositions of the studied samples.

The 30 min annealing of sample AP7(30) at 100 °C leads to the growth of the oxygen concentration on the surface (AP7c(30)) and does not affect significantly the oxygen coefficient k_O compared to AP7(20) (Table 1). The U 5f peak FWHM does not change and the peak shifts towards the higher BE range (Table 2), while $\Gamma(U\ 4f_{7/2})$ does not change much.

The further $30 \times 3 = 90$ min annealing of sample AP7c(30) at 150, 200 and 250 °C leads to changes in the oxygen concentration on the surface of sample AP7d(30), the oxygen coefficient is comparable to the k_O in sample AP7c(30) (Table 1). The U 5f peak narrowed (Table 2), while $\Gamma(U\ 4f_{7/2})$ did not change.

The considered data show that annealing at 100–250 °C after Ar^+ etching does not lead to any significant changes of the oxygen coefficient and ionic composition of the UO_{2+x} film. The etching leads to formation of self-organized stable UO_{2+x} phase with oxygen coefficient $k_O \approx 2.12$ resulting from the surface relaxation in the vacuum. Practically, on the surface (~5 nm [31]) of single crystal UO_2 film the structure UO_2 (CaF_2) was not observed. A stable oxide $UO_{2.12}$ forms on the surface. These data agree with the results of the study of (111) UO_2 single crystal surface [48].

According to the goal of this investigation, the main XPS parameters described in Introduction were studied. Thus, the measured mean U $4f_{7/2}$ BE being 380.0 eV and the mean O 1s BE being 530.1 eV (Table 2) are in a good agreement with the data in Ref. [11]. The OVMO and IVMO structures being typical for uranium dioxide (Fig. 3) agree well with the relativistic calculation results [39] and the data of other studies [20]. The mean shake-up satellite position 6.9 eV and intensity 28% agree with the data of other work [11]. Since uranium U^{4+} ion outer electron configuration is $6s^26p^65f^2$, the presence of two uncoupled U 5f electrons must lead to the multiplet splitting and widening of the core peaks like the U 4f one [28]. For the U^{6+} ions with the configuration $U^{6+}6s^26p^65f^0$ not containing the U 5f electrons such a splitting is absent in the U 4f XPS. In this case the U $4f_{7/2}$ FWHMs for $BaU^{6+}O_4$, $PbU^{6+}O_4$ and $Bi_2U^{6+}O_6$ are 1.2, 1.1 and 1.2 eV, respectively [46]. The U $4f_{7/2}$ FWHM for etched and annealed samples is higher (Fig. 8, Table 2). One of the reasons of the U 5f peak widening after the etching and narrowing after the annealing of the AP7(0) sample can be the disappearance of the U^{5+} ions with the configuration $U^{5+}6s^26p^65f^1$ after the etching and their appearance after the annealing.

4. Conclusions

The XPS study of the (111) UO_{2+x} single crystal film surface (sample AP7(0)) on a YSZ (111) substrate was carried out. The film was studied before and after the Ar^+ etching and annealing (in situ) at various times of etching and annealing.

XPS determination of the oxygen coefficient $k_O = 2 + x$ of oxide UO_{2+x} formed on the UO_2 film surface was performed on the basis of the U 4f and O 1s core-electron peak intensities, as well as on the basis of the dependence of the U 5f relative intensity on $k_O = 2 + x$ for synthetic and natural uranium oxides.

The short-time Ar^+ etching of the AP7(0) surface removes the excessive oxygen and forms the stable self-organized phase until the oxygen coefficient remains $k_O \geq 2.0$. The evaluation yields for this phase the $k_O \approx 2.12$. On the basis of the spectral parameters (binding energy; structure of the inner and outer valence molecular orbitals; intensities and position of shake-up satellites; intensities and widths of the U 4f, U 5f and O 1s peaks) one can conclude that this phase ($UO_{2.12}$) contains mostly the U^{4+} and U^{5+} ions with some U^{6+} ions also present.

Acknowledgements

The work was supported by the RFBR grant 17-03-00277a. This work was supported in part by Lomonosov Moscow State University Program of Development. A.J. Popel acknowledges funding from the UK EPSRC (grants EP/I036400/1 and EP/L018616/1) and Radioactive Waste Management Ltd (formerly the Radioactive Waste Management Directorate of the UK Nuclear Decommissioning Authority, contract NPO004411A-EPS02).

References

[1] A.L. Smirnov, V.N. Rychkov, A.B. Umanskii, E.A. Galyanina, A.M. Klyushnikov, Laws of Underground Leaching of Uranium from Ores of Hydrogenic Uranium D Kinetic features of underground uranium leaching from ores of hydrogeneous uranium deposits, Radiochemistry 51 (2009) 61–63.
[2] H. He, Z. Qin, D.W. Shoesmith, Characterizing the relationship between hyperstoichiometry, defect structure and local corrosion kinetics of uranium dioxide, Electrochim. Acta 56 (2010) 53–60.
[3] Hj. Matzke, Radiation damage-enhanced dissolution of UO_2 in water, J. Nucl. Mater. 190 (1992) 101–106.
[4] K.-U. Ulrich, E.S. Ilton, H. Veeramani, J.O. Sharp, R. Bernier-Latmani, E.J. Schofield, J.R. Bargar, D.E. Giammar, Comparative dissolution kinetics of biogenic and chemogenic uraninite under oxidizing conditions in the presence of carbonate, Geochim. Cosmochim. Acta 73 (2009) 6065–6083.
[5] K. Opel, S. Weiß, S. Hübener, H. Zänker, G. Bernhard, Study of the solubility of amorphous and crystalline uranium dioxide by combined spectroscopic methods, Radiochim. Acta 95 (2007) 143–149.
[6] H. He, R.K. Zhu, Z. Qin, P. Keech, Z. Ding, D.W. Shoesmith, Determination of local corrosion kinetics on hyper-stoichiometric UO_{2+x} by scanning electrochemical microscopy, J. Electrochem. Soc. 156 (2009) C87–C94.
[7] D.W. Shoesmith, S. Sunder, The prediction of nuclear fuel (UO_2) dissolution rates under waste disposal conditions, J. Nucl. Mater. 190 (1992) 20–35.
[8] Yu.M. Dymkov, The nature of uraninite, in: questions of genetic mineralogy, Atomizdat Moscow (1973) (in Russian).
[9] Yu. A. Teterin, A.J. Popel, K.I. Maslakov, A. Yu. Teterin, K.E. Ivanov, S.N. Kalmykov, R. Springell, T.B. Scott, I. Farnan, XPS study of ion irradiated and unirradiated UO_2 thin films, Inorg. Chem. 55 (2016) 8059–8070.
[10] H.Y. Geng, Y. Chen, Y. Kaneta, M. Kinoshita, Stability mechanism of cuboctahedral clusters in UO_{2+x}: First-principles calculations, Phys. Rev. B 77 (2008) 180101(R).
[11] H. Idriss, Surface reactions of uranium oxide powder, thin films and single crystals, Surf. Sci. Rep. 65 (2010) 67–109.
[12] M.M. Strehle, B.J. Heuser, M.S. Elbakhshwan, X. Han, D.J. Gennardo, H.K. Pappas, H. Ju, Characterization of single crystal uranium-oxide thin films grown via reactive-gas magnetron sputtering on yttria-stabilized zirconia and sapphire, Thin Solid Films 520 (2012) 5616–5626.
[13] Q. Chen, X. Lai, B. Bai, M. Chu, Structural characterization and optical properties of UO_2 thin films by magnetron sputtering, Appl. Surf. Sci. 256 (2010) 3047–3050.
[14] Z. Bao, R. Springell, H.C. Walker, H. Leiste, K. Kuebel, R. Prang, G. Nisbet, S. Langridge, R.C.C. Ward, T. Gouder, R. Caciuffo, G.H. Lander, Antiferromagnetism in UO_2 thin epitaxial films, Phys. Rev. B 88 (2013) 134426.
[15] A.J. Popel, A.M. Adamska, P.G. Martin, O.D. Payton, G.I. Lampronti, L. Picco, L. Payne, R. Springell, T.B. Scott, I. Monnet, C. Grygiel, I. Farnan, Structural effects in UO_2 thin films irradiated with U ions, Nucl. Instr. Meth. Phys. Res. B 386 (2016) 8–15.
[16] A.J. Popel, V.A. Lebedev, P.G. Martin, A.A. Shiryaev, G.I. Lampronti, R. Springell, S.N. Kalmykov, T.B. Scott, I. Monnet, C. Grygiel, I. Farnan, Structural effects in UO_2 thin films irradiated with fission-energy Xe ions, J. Nucl. Mater. 482 (2016) 210–217.
[17] J.R. Naegele, J. Ghijsen, L. Manes, Localization and hybridization of 5f states in the metallic and ionic bond as investigated by photoelectron spectroscopy, Struct. Bond. 59/60 (1985) 197–262.
[18] A. Seibert, T. Gouder, F. Huber, Formation and stability of actinide oxides: a valence band photoemission study, Radiochim. Acta 97 (2009) 247–250.
[19] T. Gouder, A. Seibert, L. Havela, J. Rebizant, Search for higher oxides of Pu: a photoemission study, Surf. Sci. 601 (2007) L77–L80.
[20] Yu. A. Teterin, A. Yu. Teterin, The structure of X-ray photoelectron spectra of light actinide compounds, Russ. Chem. Rev. 73 (2004) 541–580.
[21] J.G. Tobin, D.K. Shuh, Electron spectroscopy of the oxidation and aging of U and Pu, J. Electron Spectrosc. Relat. Phenom. 205 (2015) 83–91.
[22] A.K. Burrell, T.M. McCleskey, P. Shukla, H. Wang, T. Durakiewicz, D.P. Moore, C.G. Olson, J.J. Joyce, Q. Jia, Controlling oxidation states in uranium oxides through epitaxial stabilization, Adv. Mater. 19 (2007) 3559–3563.
[23] S. Stumpf, A. Seibert, T. Gouder, F. Huber, T. Wiss, J. Römer, Development of fuel-model interfaces: investigations by XPS, TEM, SEM and AFM, J. Nucl. Mater. 385 (2009) 208–211.
[24] J.C. Fuggle, N. Ma°rtenson, Core-level binding energy in metals, J. Electron Spectrosc. Relat. Phenom. 21 (1980) 275–281.
[25] E.S. Ilton, P.S. Bagus, XPS determination of uranium oxidation states, Surf. Interface Anal. 43 (2011) 1549–1560.
[26] Yu. A. Teterin, M.V. Ryzhkov, A. Yu. Teterin, A.D. Panov, A.S. Nikitin, K.E. Ivanov, I.O. Utkin, X-ray spectroscopic study of U 6p,5f electronic levels in γ-UO_3, Radiochemistry 44 (2002) 224–233.
[27] E.S. Ilton, P.S. Bagus, Many-body effects in the 4*f* x-ray photoelectron spectroscopy of the U^{5+} and U^{4+} free ions, Phys. Rev. B 71 (2005) 195121.
[28] E.S. Ilton, P.S. Bagus, Ligand field effects on the multiplet structure of the U4f XPS of UO_2, Surf. Sci. 602 (2008) 1114–1121.
[29] E.S. Ilton, A. Haiduc, C.L. Cahill, A.R. Felmy, Mica surfaces stabilize pentavalent uranium, Inorg. Chem. 44 (2005) 2986–2988.
[30] V.G. Yarzhemsky, M.Y. Amusia, Calculation of Ar photoelectron satellites in the hard-x-ray region, Phys. Rev. A 93 (2016) 063406.
[31] A. Yu. Teterin, Yu. A. Teterin, K.I. Maslakov, O.N. Batuk, S.N. Kalmykov, E.V. Zakharova, Determination of the ionic composition and oxidation state of uranium on the surface of oxides UO_{2+x} from the XPS data, Radiochemistry 51 (2009) 450–457.
[32] S.D. Senanayake, H. Idriss, UO_2 (111) single crystal: comparison of stoichiometric and defective surfaces by XPS, Surf. Sci. Spec. 13 (2006) 72–80.
[33] S.V. Chong, M.A. Barteau, H. Idriss, Stoichiometric and Ar-ion sputtered uranium dioxide (111) single crystal by XPS, Surf. Sci. Spec. 8 (2001) 297–302.
[34] S.D. Senanayake, A. Soon, A. Kohlmeyer, T. Söhnel, H. Idriss, Carbon monoxide reaction with UO_2 (111) single crystal surfaces: a theoretical and experimental study, J. Vac. Sci. Technol. A 23 (2005) 1078–1084.
[35] D. Shirley, High-resolution X-ray photoemission spectrum of the valence bands of gold, Phys. Rev. B 5 (1972) 4709–4714.
[36] V.V. Nemoshkalenko, V.G. Aleshin, X-Ray Photoelectron Spectroscopy of Crystals, Naukova Dumka, Kiev, 1976 (in Russian).
[37] T. Gouder, L. Havela, Examples of quantification in XPS on 5f materials, Mikrochim. Acta 138 (2002) 207–215.
[38] V.I. Nefedov, X-ray Photoelectron Spectroscopy of Chemical Compounds, Himiya, Moscow, 1984 (in Russian).
[39] Yu. A. Teterin, K.I. Maslakov, M.V. Ryzhkov, O.A. Traparić, L. Vukčević, A. Yu. eterin, A.D. Panov, Nature of the chemical bond in uranium dioxide UO_2, Radiochemistry 47 (2005) 215–224.
[40] I.M. Band, Y.I. Kharitonov, M.B. Trzhaskovskaya, Photoionization cross sections and photoelectron angular distributions for x-ray line energies in the range 0. 132–4.509 keV targets: $1 \leq Z \leq 100$, Atom. Data Nucl. Data 23 (1979) 443–505.
[41] Yu.A. Teterin, A.S. Baev, S.G. Gagarin, A.P. Kovtun, Peculiarities of XPS spectra of elements of VIA group, Dokl. Akad. Nauk SSSR (Rep. Acad. Sci. USSR) 273 (1983) 56–160 (in Russian).
[42] R.P. Rafalsky, V.A. Alexeev, L.A. Ananyeva, Phase composition of synthetic and natural uranium oxides, Geokhimiya (Geochemistry) 11 (1979) 1601–1615 (in Russian).
[43] Yu. A. Teterin, A. Yu. Teterin, K.E. Ivanov, M.V. Ryzhkov, S.N. Maslakov, V.G. Petrov, D.A. Enina, X-ray photoelectron spectra structure and chemical bond nature in NpO_2, Phys. Rev. B 89 (2014) 035102.
[44] Yu. A. Teterin, K.I. Maslakov, A.Yu. Teterin, K.E. Ivanov, M.V. Ryzhkov, V.G. Petrov, D.A. Enina, S.N. Kalmykov, Electronic structure and chemical bonding in PuO_2, Phys. Rev. B 87 (2013) 245108.
[45] Yu. A. Teterin, K.I. Maslakov, M.V. Ryzhkov, A. Yu. Teterin, K.E. Ivanov, S.N. Kalmykov, V.G. Petrov, X-ray photoelectron spectra structure and chemical bonding in AmO_2, Nucl. Technol. Radiat. 30 (2015) 83–98.
[46] D.O. Charkin, S.M. Kazakov, S.N. Kalmykov, A.V. Gorbachev, A.N. Kuznetsov, A. Yu. Zakharov, Yu. A. Teterin, K.I. Maslakov, A. Yu. Teterin, K.E. Ivanov, Synthesis and XPS studies of uranium-bearing Aurivillius-derived layered perovskites, J. Alloys Compd. 677 (2016) 271–280.
[47] W. Breitung, Oxygen self and chemical diffusion coefficients in $UO_{2\pm x}$, J. Nucl. Mater. 74 (1978) 10–18.
[48] J.E. Stubbs, A.M. Chaka, E.S. Ilton, C.A. Biwer, M.H. Engelhard, J.R. Bargar, P.J. Eng, UO(2) oxidative corrosion by nonclassical diffusion, Phys. Rev. Lett. 114 (2015) 246103.
[49] M.N. Hedhili, B.V. Yakshinskiy, T.E. Madey, Interaction of water vapor with UO_2(001), Surf. Sci. 445 (2000) 512–525.